IEEE Sensors Letters VOL. 7, NO. 2, FEBRUARY 2023

IEEE Sensors Council

Sensor networks

Flying Path Optimization of Rechargeable UAV for Data Collection in Wireless Sensor Networks

Yuchao Zhu* and Shaowei Wang**

School of Electronic Science and Engineering, Nanjing University, Nanjing 210023, China
**Graduate Student Member, IEEE*
***Senior Member, IEEE*

Manuscript received 27 December 2022; accepted 13 January 2023. Date of publication 17 January 2023; date of current version 31 January 2023.

Abstract—In this letter, we study a novel framework to realize efficient data collection from wireless sensor networks, where an unmanned aerial vehicle (UAV) is dispatched to collect the aggregated data from cluster heads and an unmanned ground vehicle carrying backup batteries moves along with the UAV to compensate for the shortage of UAV energy. Our optimization task is to minimize the mission time of a complete round of data collection, which is formulated as a coordinated traveling salesman problem with battery constraints and is solved by a heuristic path planning algorithm. Numerical results show that our proposal outperforms compared methods under appropriate configuration.

Index Terms—Sensor networks, data collection, path planning, unmanned aerial vehicle (UAV), wireless sensor network.

I. INTRODUCTION

Composed of numerous tiny size, low-power, and inexpensive sensor nodes, wireless sensor networks (WSNs) have been widely used for constructing cyber-physical systems in inaccessible areas [1]. Emerging applications, such as battlefield surveillance, environmental monitoring, and precision agriculture require efficient and reliable data collection to enable remote control of WSNs [2]. Traditional frameworks of data collection from WSNs include multihop routing networks and unmanned ground vehicle (UGV) assisted routing networks [3], [4]. However, the former is unreliable since it is influenced by the wireless links between sensor nodes, and the latter is inefficient since some areas are dangerous and unreachable for UGVs.

Due to the high mobility, fast deployment, and strong line-of-sight links, unmanned aerial vehicles (UAVs) can act as aerial mobile sinks to enable swift and reliable data collection in WSNs [5], [6], [7]. Since letting the UAV directly communicates with each sensor node will lead to the high energy consumption of both the UAV and sensor nodes, cluster heads (CHs) are deployed to aggregate the collected data and the UAV generally communicates with the CHs [8]. In [9], a hierarchical clustering-based data collection scheme is presented to mitigate the energy hole in WSNs. In [10], an adaptive modulation scheme is adopted to improve the energy efficiency of sensors while guaranteeing the fairness between different CHs. To avoid collision caused by simultaneous transmission and improve transmission efficiency, authors in [11] propose a priority-based data access strategy with the consideration of UAV's mobility. Considering the energy consumption of both the UAV and the WSN, the selection of CHs and the flying path of the UAV are jointly optimized by deep reinforcement learning in [12]. The multi-UAV enabled data collection mission is considered in [13], where the number of UAVs and their trajectories are optimized by solving a capacitated vehicle routing problem. In [14], a multiagent deep reinforcement learning with long short-term memory is developed to design the trajectories and patrol speeds of the UAVs and their data aggregation schedules, by which the buffer overflows at the ground nodes and communication failures are minimized.

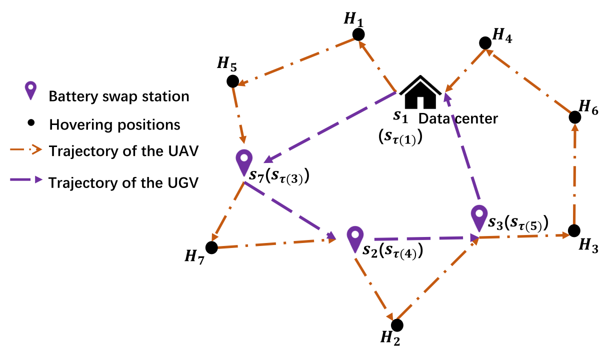

Fig. 1. UAV and UGV assisted data collection for WSN.

Although UAVs play a powerful role in gathering data from WSNs, the service range of UAVs is limited that they are unable to travel long distances or operate for long periods of time due to the finite onboard energy. Recent works envisage that the UAV's battery can be recharged or replaced whenever used up during its flight [15], [16]. To this end, we investigate a promising UAV-UGV-assisted data collection scheme to minimize the complete-round mission time, where the UAV flies to and hovers above the CHs for data collection, and the UGV carrying backup batteries moves together with the UAV to provide on-demand self-recharging. The key points are determining when and where the UAV and UGV should rendezvous with each other. Due to the NP-hardness of the task, we develop a heuristic four-step algorithm to jointly plan the paths of the UAV and the UGV.

II. SYSTEM MODEL AND PROBLEM FORMULATION

A. Network Description

As depicted in Fig. 1, we consider a WSN located in region $\mathcal{R} \in \mathbb{R}^2$ with side length L, consisting of one data center $\boldsymbol{d}_0$, one UGV,

Corresponding author: Shaowei Wang (e-mail: wangsw@nju.edu.cn).
Associate Editor: F. Falcone.
Digital Object Identifier 10.1109/LSENS.2023.3237634

one rotary-wing UAV and M CHs. The set of CHs is denoted by $\mathcal{C} = \{1, 2, \ldots, M\}$, where the location of CH $i \in \mathcal{C}$ is $\boldsymbol{c}_i = (c_i^x, c_i^y, 0)$. In our system, the UAV hovers above the CHs to collect the aggregated data. According to the air-to-ground channel model [17], the altitude of the UAV could be adjusted to achieve different transmission rates. Without loss of generality, we set a fixed flying altitude h and the hovering positions of the UAV are denoted by $\mathcal{H} = \{H_i | H_i = (c_i^x, c_i^y, h), i \in \mathcal{C}\}$. The UAV needs to fly back to the moving UGV for battery replenishment when its energy is about to run out. The candidates of locations at which they rendezvous with each other are denoted by "battery swap station" (BSS) $\mathcal{S} = \{\boldsymbol{s}_i | \boldsymbol{s}_i = (s_i^x, s_i^y, 0), i \in \mathcal{C}\}$. The set of permutations of $\mathcal{C}$ is denoted by U_M, and a particular permutation is denoted by $\tau \in U_M$, with the added convention that $\tau(M+1) = \tau(1)$ for notation convenience (e.g., $\tau = \{1, 5, 7, 2, 3, 6, 4, 1\}$ in Fig. 1).

B. Problem Formulation

The velocity of the UGV and UAV are denoted by $v_0, v_1 > 0$ (with $v_0 < v_1$), respectively. The energy consumption of flying and hovering are e_f and e_h, respectively, and the capacity of the battery is denoted by E. Note that e_h depends on the hovering time above each CH, we set the hovering time as 1 without loss of generality.

Define $E_{\tau(k)}|_{k \in \mathcal{C}}$ as the remaining energy at $H_{\tau(k)}$, which can be mathematically written as follows based on the fact whether the UAV has replaced its battery or not

$$E_{\tau(k)} = \begin{cases} E - e_h - \frac{e_f \|H_{\tau(k)} - \boldsymbol{s}_{\tau(k)}\|}{v_1}, & \text{if } z_{\tau(k)} = 1 \\ E - e_h \left(\sum_{j=l_k}^{k} \left(1 - z_{\tau(j)}\right) + 1 \right) - \frac{e_f d_{\tau(k)}}{v_1}, & \text{otherwise} \end{cases} \tag{1}$$

where $d_{\tau(k)}$ is the continuous flying distance for the UAV to reach the kth hovering position, and the binary variable $z_{\tau(k)}|_{k \in \mathcal{C}}$ indicates whether the kth BSS is needed or not

$$z_{\tau(k)} = \begin{cases} 1, \text{if } k = 1 \text{ or } E_{\tau(k-1)} < \frac{e_f \|H_{\tau(k)} - H_{\tau(k-1)}\|}{v_1} + e_h \\ 0, \text{otherwise} \end{cases} \tag{2}$$

and the corresponding locations of BSSs can be expressed as

$$\boldsymbol{s}_{\tau(k)} = \begin{cases} \boldsymbol{d}_0, & \text{if } k = 1 \\ \boldsymbol{s}_{\tau(k)}, & \text{if } z_{\tau(k)} = 1 \\ \boldsymbol{s}_{\tau(k-1)}, & \text{otherwise.} \end{cases} \tag{3}$$

Let $\boldsymbol{s}_{\tau(l_k)}$ with $l_k = \max_{a=1,2,\ldots,k} a|_{z_{\tau(a)}=1}$ denote the closest BSS to the kth hovering position, thus, the continuous flight distance $d_{\tau(k)}$ can be expressed as

$$d_{\tau(k)} = \|\boldsymbol{s}_{\tau(l_k)} - H_{\tau(l_k)}\| + \sum_{j=l_k}^{k} \left(1 - z_{\tau(j)}\right) \|H_{\tau(j-1)} - H_{\tau(j)}\|. \tag{4}$$

We focus on the completion time of data collection since the mission is delay-tolerant. As shown in Fig. 1, the complete tour can be divided into $m = \sum_{k=1}^{M} z_{\tau(k)}$ subtours, denoted by $\mathcal{M} = \{1, 2, \ldots, m\}$. The flight that the UAV takes off from one BSS, gathers data from CHs, and lands on the next BSS is regarded as a subtour. Thus, the UAV's flying distance of the bth subtour can be written as

$$d_{\text{uav}}^b = \|\boldsymbol{s}_{\tau(\Omega(b))} - H_{\tau(\Omega(b))}\| + \|H_{\tau(\Omega(b+1)-1)} - \boldsymbol{s}_{\tau(\Omega(b+1))}\| + \sum_{j=\Omega(b)}^{\Omega(b+1)-2} \|H_{\tau(j)} - H_{\tau(j+1)}\| \tag{5}$$

where $\Omega = \{k | z_{\tau(k)} = 1, 1 \le k \le M+1\}$ is the set of indexes of needed BSSs (e.g., $\Omega = \{1, 3, 4, 5, 8\}$ in Fig. 1). And the UGV's moving distance on the corresponding subtour can be written as

$$d_{\text{ugv}}^b = \|\boldsymbol{s}_{\tau(\Omega(b))} - \boldsymbol{s}_{\tau(\Omega(b+1))}\|. \tag{6}$$

The key point of our optimization task is to find the optimal locations of BSSs, which can be formulated as follows:

$$\begin{aligned} &\underset{\tau \in U_M, \mathcal{S}, z_{(\cdot)}}{\text{minimize}} \quad \sum_{b=1}^{m} \max \left\{ \frac{d_{\text{uav}}^b}{v_1}, \frac{d_{\text{ugv}}^b}{v_0} \right\} \\ &\text{s.t. } C_1 : \frac{d_{\text{uav}}^b e_f}{v_1} + (\Omega(b+1) - \Omega(b))\, e_h \le E \quad \forall b \in \mathcal{M} \\ &\quad C_2 : z_n \in \{0, 1\} \quad \forall n \in \mathcal{C}. \end{aligned} \tag{7}$$

The constraint C_1 guarantees that the UAV can return to the UGV in each subtour. Problem (7) can be regarded as an extension of the Euclidean traveling salesman problem (TSP) that requires considering the paths of both the UAV and UGV, which is NP-hard.

III. PROPOSED PATH PLANNING ALGORITHM

The key points of (7) lie in determining when and where the UAV and UGV rendezvous with each other. Note that, the task can be transformed into the following convex problem when given the visiting sequence τ and the set of needed BSSs Ω:

$$\begin{aligned} &\underset{\mathcal{S}, t_{(\cdot)}}{\text{minimize}} \quad t_{m+1} \\ &\text{s.t. } C_1 : t_{i+1} \ge t_i + \frac{\|\boldsymbol{s}_{\Omega(i)} - \boldsymbol{s}_{\Omega(i+1)}\|}{v_0} \quad \forall i \in \mathcal{C} \\ &\quad C_2 : t_{i+1} \ge t_i + \frac{d_{\text{uav}}^i}{v_1} \quad \forall i \in \mathcal{C} \\ &\quad C_3 : \frac{d_{\text{uav}}^i}{v_1} < \frac{E - e_h\,(\Omega(i+1) - \Omega(i))}{e_f} \quad \forall i \in \mathcal{C} \\ &\quad C_4 : t_1 = 0 \\ &\quad C_5 : \boldsymbol{s}_1 = \boldsymbol{s}_{M+1} = \boldsymbol{d}_0 \end{aligned} \tag{8}$$

where $d_{\text{uav}}^i = \sum_{j=\Omega(i)}^{\Omega(i+1)-2} \|H_j - H_{j+1}\| + \|\boldsymbol{s}_{\Omega(i)} - H_{\Omega(i)}\| + \|H_{\Omega(i+1)-1} - \boldsymbol{s}_{\Omega(i+1)}\|$ according to (5), $t_{(\cdot)}$ denotes the accumulative time at the end of each subtour. Thus, we propose a heuristic algorithm called LKH-SC to address (7), which is described in Algorithm 1.

In Step 1, set the battery constraints aside, we use a classical algorithm called LKH [18] to solve the TSP tour of $\mathcal{H}$ and get the visiting sequence τ. Then, the locations of BSSs and mission completion time are calculated under the initial setting that $z_{(\cdot)} = 1$. Next, based on the initial locations of BSSs, the remaining energy at each hovering position and $z_{(\cdot)}$ are updated successively. Finally, we update the corresponding locations of BSSs, and the coordinated paths can be found.

IV. NUMERICAL RESULTS

Consider a square area with side length L km, where CHs are uniformly deployed and the data center is located at $\boldsymbol{d}_0 = [0, 0]$ m. The flying altitude of the UAV is set as $h = 100$ m. The battery parameters of the UAV are $e_f = 5$ W, $e_h = 10$ Wh, and $E = 40$ Wh, respectively. Unless otherwise specified, the velocity of UGV and UAV are set as $v_0 = 15$ km/h and $v_1 = 60$ km/h, respectively.

We compare our selective-charging scheme with five other methods adopting different path planning and recharging strategies. LKH-FC is a fully charging strategy based on the TSP tour solved by LKH,

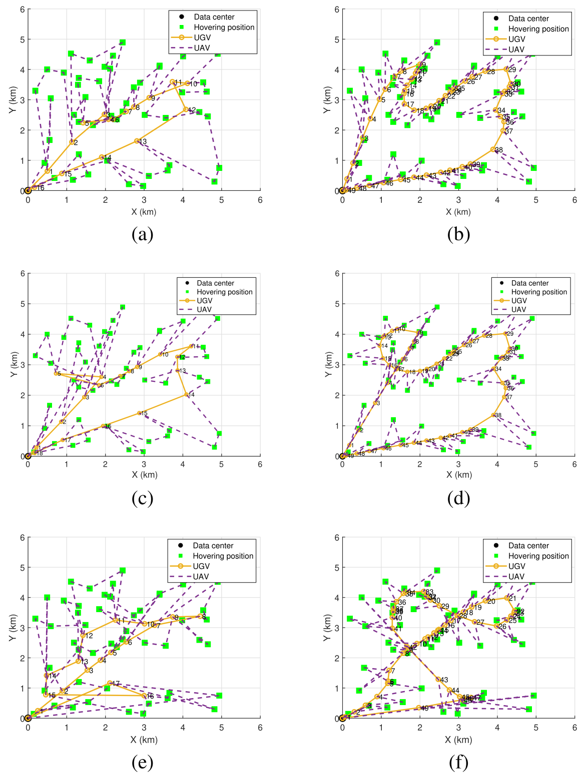

Fig. 2. Path planning results by different methods under an instance of $M = 50$, $L = 5$ km. (a) LKH-SC. (b) LKH-FC. (c) ACO-SC. (d) ACO-FC. (e) NN-SC. (f) NN-FC.

Algorithm 1: LKH-SC.

1: **Input**: Target region $\mathcal{R}$, cluster heads $\mathcal{C}$, hovering positions $\mathcal{H}$, parameters of UGV and UAV: v_0, v_1, e_f, e_h, E.
2: Initialization: $z_{(\cdot)} = 1$, $\Omega = \{1, 2, \ldots, M+1\}$.
3: **Step 1**: Use LKH algorithm to solve the TSP tour of $\mathcal{H}$;
4: Return τ, set $z^*_{(\cdot)} \leftarrow z_{(\cdot)}$, $\Omega^* \leftarrow \Omega$,;
5: **Step 2**: Use CVX to solve problem (8) under τ and Ω^*;
6: Return initial locations of BSSs: $\mathcal{S}^* \leftarrow \mathcal{S}$, initial completion time: $t^*_{m+1} \leftarrow t_{m+1}$;
7: **Step 3**: Calculate $E_{(\cdot)}$ and $z_{(\cdot)}$ by (1) and (2);
8: Update Ω according to $z_{(\cdot)}$: $\Omega^{temp} \leftarrow \Omega$;
9: **Step 4**: Use CVX to solve problem (8) under τ and Ω^{temp};
10: **if** $t_{m+1} < t^*_{m+1}$ **then**
11: $\mathcal{S}^* \leftarrow \mathcal{S}$, $z^*_{(\cdot)} \leftarrow z_{(\cdot)}$, $\Omega^* \leftarrow \Omega$, $t^*_{m+1} \leftarrow t_{m+1}$;
12: **else**
13: $\mathcal{S}^*$, $z^*_{(\cdot)}$, Ω^*, t^*_{m+1} do not change;
14: **end if**
15: **Output**: τ, $\mathcal{S}^*$, t^*_{m+1}.

where the UAV flies back to the UGV for battery replenishment after each hovering regardless of its remaining energy, which is a special case ($z_{(\cdot)} = 1$) of LKH-SC. ACO-FC and ACO-SC are fully charging and selective-charging strategies based on the TSP tour solved by ant colony optimization [19], respectively. NN-FC and NN-SC are fully charging and selective-charging strategies based on the nearest-neighbor tour, respectively. Unless otherwise specified, all results are averaged over 50 Monte Carlo simulations.

Taking a randomly generated sample of $M = 50$ and $L = 5$ km as an example, we first present in Fig. 2 the path planning results by different methods. We can observe that the UGV takes a shorter path by the selective-charging scheme as compared with the fully charing scheme, which indicates that the selective-charging scheme can exploit the agility of the UAV. In addition, there exist lots of twists and turns in the paths obtained by the ACO-based and NN-based methods, which are inefficient as compared with the relatively smooth paths obtained by the LKH-based methods.

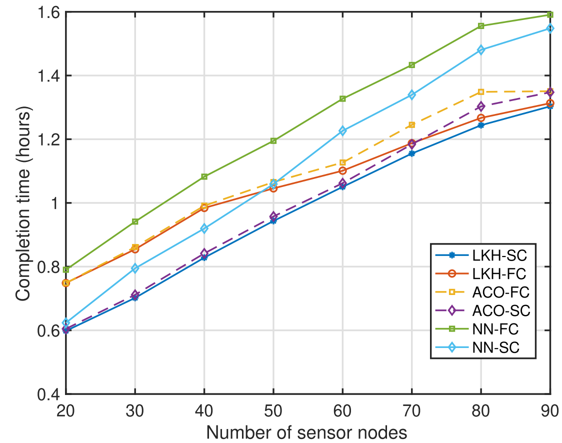

Fig. 3. Completion time as a function of the number of CHs, $L = 5$ km.

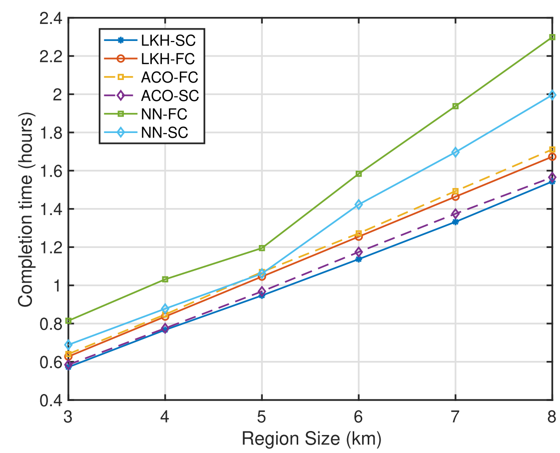

Fig. 4. Completion time as a function of the region size, $M = 50$.

We then investigate the system performance as a function of the number of CHs in Fig. 3. As expected, the completion time is roughly in a linear relationship with the number of CHs. The LKH-based schemes significantly outperform the corresponding NN-based schemes since the paths found by LKH-based schemes are shorter than that of NN-based schemes. We can also observe that LKH-based schemes perform slightly better than ACO-based schemes, and the performance gap increases as the number of sensor nodes becomes larger. This is reasonable since ACO is a meta-heuristic algorithm whose performance is greatly influenced by the hyperparameters. Our proposed LKH-SC is more efficient than the LKH-FC when the number of CHs is relatively small, while the performance approaches that of LKH-FC as the number of CHs increases (e.g., $M > 70$). The reason is that the length of an optimal TSP tour of a set of points follows a law of large numbers, the selective-charging scheme can not achieve additional gain by saving traveling time when the number of CHs is large.

Fig. 4 shows the mission completion time as a function of region size, which also follows a linear relationship. As the region becomes larger, the advantage of our proposed LKH-SC scheme becomes bigger.

In Fig. 5, we present the completion time as a function of $\frac{v_1}{v_0}$. It also can be seen that LKH-based schemes perform better than ACO-based

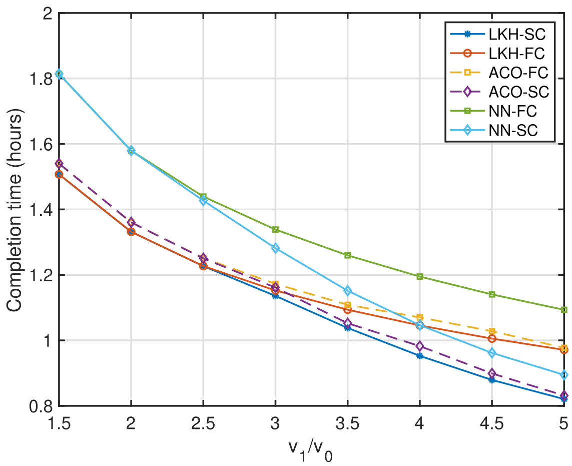

Fig. 5. Completion time as a function of v_1/v_0, $v_0 = 15$ km/h, $M = 50$.

and NN-based. We can observe that the performance gap between our proposal and LKH-FC is negligible when $v_1/v_0 < 2.5$, while the advantage of our proposal becomes larger as the ratio of v_1 and v_0 becomes larger. This is reasonable that the UGV in a selective-charging strategy inevitably consumes more time waiting for rendezvousing with the UAV when the speed of the UAV is close to the UGV. Fig. 5 indicates that the appropriate configuration of the UAV and UGV speed is important in practice.

V. CONCLUSION

In this letter, we investigated the UAV-assisted data collection in WSNs, where a UGV was introduced to realize the on-demand self-recharging of the UAV. Aiming at gathering data swiftly under the UAV battery constraint, a selective-charging strategy based on the TSP tour was proposed to optimize the time and location that the UAV and UGV rendezvous with each other. Numerical results show that our proposal can provide a guideline for data collection design in practice.

ACKNOWLEDGMENT

The authors would like to thank the editors and the anonymous reviewers, whose invaluable comments helped improve the presentation of this letter substantially. This work was supported by the National Natural Science Foundation of China under Grant 61931023 and Grant U1936202.

REFERENCES

[1] T. O. Olasupo, "Wireless communication modeling for the deployment of tiny IoT devices in rocky and mountainous environments," *IEEE Sensors Lett.*, vol. 3, no. 7, pp. 3–6, Jul. 2019, Art. no. 6001204.

[2] H. Xie, Z. Yan, Z. Yao, and M. Atiquzzaman, "Data collection for security measurement in wireless sensor networks: A survey," *IEEE Internet Things J.*, vol. 6, no. 2, pp. 2205–2224, Nov. 2019.

[3] J. Yick, B. Mukherjee, and D. Ghosal, "Wireless sensor network survey," *Comput. Netw.*, vol. 52, no. 12, pp. 2292–2330, 2008.

[4] L. He, J. Pan, and J. Xu, "A progressive approach to reducing data collection latency in wireless sensor networks with mobile elements," *IEEE Trans. Mob. Comput.*, vol. 12, no. 7, pp. 1308–1320, Jul. 2013.

[5] Y. Lin, T. Wang, and S. Wang, "UAV-assisted emergency communications: An extended multi-armed bandit perspective," *IEEE Commun. Lett.*, vol. 23, no. 5, pp. 938–941, Mar. 2019.

[6] Y. Zhu and S. Wang, "Aerial data collection with coordinated UAV and truck route planning in wireless sensor network," in *Proc. IEEE GLOBECOM'21*, Madrid, Spain, 2021, pp. 1–6.

[7] H. Kurunathan et al., "Machine learning-aided operations and communications of unmanned aerial vehicles: A contemporary survey," 2022, *arXiv:2211.04324*.

[8] W. Dargie and J. Wen, "A simple clustering strategy for wireless sensor networks," *IEEE Sensors Lett.*, vol. 4, no. 6, Jun. 2020, Art. no. 7500804.

[9] P. K. Donta, B. S. P. Rao, T. Amgoth, C. S. R. Annavarapu, and S. Swain, "Data collection and path determination strategies for mobile sink in 3D WSNs," *IEEE Sensors J.*, vol. 20, no. 4, pp. 2224–2233, Feb. 2020.

[10] A. E. Abdulla et al., "An optimal data collection technique for improved utility in UAS-aided networks," in *Proc. IEEE INFOCOM'14*, Toronto, ON, Canada, 2014, pp. 736–744.

[11] S. Say, H. Inata, J. Liu, and S. Shimamoto, "Priority-based data gathering framework in UAV-assisted wireless sensor networks," *IEEE Sensors J.*, vol. 16, no. 14, pp. 5785–5794, Jul. 2016.

[12] B. Zhu, E. Bedeer, H. H. Nguyen, R. Barton, and J. Henry, "UAV trajectory planning in wireless sensor networks for energy consumption minimization by deep reinforcement learning," *IEEE Trans. Veh. Technol.*, vol. 70, no. 9, pp. 9540–9554, Sep. 2021.

[13] O. Ghdiri et al., "Energy-efficient multi-UAV data collection for IoT networks with time deadlines," in *Proc. IEEE Glob. Commun. Conf.*, Taibei, China, 2020, pp. 1–6.

[14] K. Li, W. Ni, Y. Emami, and F. Dressler, "Data-driven flight control of internet-of-Drones for sensor data aggregation using multi-agent deep reinforcement learning," *IEEE Wireless Commun.*, vol. 29, no. 4, pp. 18–23, Aug. 2022.

[15] Y. Wang, Z. Su, N. Zhang, and R. Li, "Mobile wireless rechargeable UAV networks: Challenges and solutions," *IEEE Commun. Mag.*, vol. 60, no. 3, pp. 33–39, Mar. 2022.

[16] Y. Zhu and S. Wang, "Efficient aerial data collection with cooperative trajectory planning for large-scale wireless sensor networks," *IEEE Trans. Commun.*, vol. 70, no. 1, pp. 433–444, Jan. 2022.

[17] A. Al-Hourani, S. Kandeepan, and S. Lardner, "Optimal LAP altitude for maximum coverage," *IEEE Wireless Commun. Lett.*, vol. 3, no. 6, pp. 569–572, Dec. 2014.

[18] K. Helsgaun, "General k-opt submoves for the Lin-Kernighan TSP heuristic," *Math. Program. Comput.*, vol. 1, no. 2/3, pp. 119–163, Jul. 2009.

[19] A. Colorni, M. Dorigo, and V. Maniezzo, "Distributed optimization by ant colonies," in *Proc. 1st Eur. Conf. Artif. Life*, 1991, pp. 134–142.